

# Calculating Far-Field Radiation Based on FEKO Spherical Wave Coefficients

Adrian Sutinjo

## I. INTRODUCTION

Numerical electromagnetic simulation packages, such as FEKO ([www.feko.info](http://www.feko.info)), most typically provide far-field data at constant  $\Delta\theta, \Delta\phi$  steps. This works fine for antenna applications, but is inconvenient in Radio Astronomy as celestial sources do not generally follow constant  $\theta$  or  $\phi$  trajectories. However, an option to calculate Spherical Wave Expansion (SWE) coefficients is provided in FEKO. This allows calculation of *continuous* (near and far) fields at radii larger than that of the sphere containing the sources [1], [2]. Radio astronomy deals with far-field radiation, and hence, a far-field expression is sufficient for our purpose.

## II. FAR-FIELD EXPRESSION USING FEKO'S SWE

We follow FEKO's SWE convention as described in [1]. In the far-field ( $r \rightarrow \infty$ ), the electric field can be expressed as:

$$\vec{E}^{\text{ff}}(r, \theta, \phi) = \beta \sqrt{\frac{Z_0}{2\pi}} \frac{e^{-j\beta r}}{\beta r} \left[ \sum_{n=1}^{\infty} \sum_{m=-n}^n \frac{e^{jm\phi} C_{mn}}{\sqrt{n(n+1)}} \left(\frac{-m}{|m|}\right)^m (e_{mn}^{\theta} \hat{\theta} + e_{mn}^{\phi} \hat{\phi}) \right] \quad (1)$$

where  $\beta$  is the wavenumber and  $Z_0$  is the intrinsic impedance of free space and

$$e_{mn}^{\theta} = Q_{1mn} j^{n+1} \frac{jm}{\sin \theta} P_n^{|m|}(\cos \theta) + Q_{2mn} j^n \frac{dP_n^{|m|}(\cos \theta)}{d\theta} \quad (2)$$

$$e_{mn}^{\phi} = Q_{2mn} j^n \frac{jm}{\sin \theta} P_n^{|m|}(\cos \theta) - Q_{1mn} j^{n+1} \frac{dP_n^{|m|}(\cos \theta)}{d\theta} \quad (3)$$

$Q_{smn}$  are the coefficients given by FEKO where  $s = 1$  and  $s = 2$  refer to TE and TM modes, respectively. Similar expressions, though with slightly different conventions, may be found in [3], [4]. Also,

$$C_{mn} = \sqrt{\frac{2n+1}{2} \frac{(n-|m|)!}{(n+|m|)!}} \quad (4)$$

is the normalization factor for the associated Legendre function of order  $n$  and rank  $|m|$ ,  $P_n^{|m|}(\cos \theta)$  [5], [6].

### A. Dealing with $P_n^{|m|}(\cos \theta)/\sin \theta$

The factor  $P_n^{|m|}(\cos \theta)/\sin \theta$  gives an *appearance* of singularity for  $\theta \rightarrow 0, \pi$  which requires special treatment. Note that  $\theta = 0$  is in the direction of the zenith in LFAA; it is important that we get this right. We can use a solution to the associated Legendre equation given by [6]:

$$P_n^{|m|}(u) = (-1)^{|m|} (1-u^2)^{|m|/2} \frac{d^{|m|} P_n(u)}{du^{|m|}} \quad (5)$$

where  $u = \cos \theta$ . It follows that

$$\begin{aligned} \frac{P_n^{|m|}(\cos \theta)}{\sin \theta} &= \frac{P_n^{|m|}(u)}{(1-u^2)^{1/2}} \\ &= (-1)^{|m|} (1-u^2)^{(|m|-1)/2} \frac{d^{|m|} P_n(u)}{du^{|m|}} \end{aligned} \quad (6)$$

There are three cases to consider:

1)  $m = 0$ : In (2) and (3) (and as it turns out, in all cases encountered here), the  $P_n^{|m|}(\cos \theta)/\sin \theta$  factor is multiplied by such that

$$m P_n(\cos \theta) / \sin \theta \xrightarrow{\theta=0, \pi} 0 \quad (7)$$

2)  $|m| = 1$ : Setting  $|m| = 1$  in (6), we obtain

$$\frac{P_n(\cos \theta)}{\sin \theta} = -\frac{dP_n(u)}{du} \quad (8)$$

From the definition of the Legendre polynomial [6]

$$P_n(u) = \sum_{l=0}^L \frac{(-1)^l (2n-2l)!}{2^n l! (n-l)! (n-2l)!} u^{n-2l} \quad (9)$$

where  $L = n/2$  (for  $n$  even) or  $(n-1)/2$  (for  $n$  odd). Therefore, we can write

$$\frac{dP_n(u)}{du} = \sum_{l=0}^L \frac{(-1)^l (2n-2l)! (n-2l)}{2^n l! (n-l)! (n-2l)!} u^{n-2l-1} \quad (10)$$

which allows us to obtain, for  $\theta \rightarrow 0, \pi$ :

$$\frac{dP_n(u)}{du} \xrightarrow{u=\pm 1} \sum_{l=0}^L \frac{(-1)^l (2n-2l)! (n-2l)}{2^n l! (n-l)! (n-2l)!} (\pm 1)^{n-2l-1} \quad (11)$$

3)  $|m| \geq 2$ : From (6), we obtain

$$P_n^{|m|}(\cos \theta) / \sin \theta = (-1)^{|m|} (\sin \theta)^{|m|-1} \frac{d^{|m|} P_n(\cos \theta)}{d(\cos \theta)^{|m|}} \quad (12)$$

Equation (9) suggests that  $P_n(u)$  is continuously differentiable for  $|u| \leq 1$ , hence

$$P_n^{|m|}(\cos \theta) / \sin \theta \xrightarrow{\theta=0, \pi} 0 \quad (13)$$

Table I summarizes our discussion in this subsection. Note that the pre-multiplying factor,  $m$ , is included.

Table I  
SUMMARY OF  $\lim_{\theta \rightarrow 0, \pi} \frac{m P_n^{|m|}(\cos \theta)}{\sin \theta}$

$ m $	$\lim_{\theta \rightarrow 0, \pi} \frac{m P_n^{ m }(\cos \theta)}{\sin \theta}$
0	0
1	$-m \sum_{l=0}^{L=\text{floor}(n/2)} \frac{(-1)^l (2n-2l)! (n-2l)}{2^n l! (n-l)! (n-2l)!} (\cos(\theta = 0, \pi))^{n-2l-1}$
$\geq 2$	0

B. Dealing with  $dP_n^{|m|}(\cos \theta)/d\theta$

We are interested in

$$\frac{dP_n^{|m|}(\cos \theta)}{d\theta} = -\sin \theta \frac{dP_n^{|m|}(\cos \theta)}{d(\cos \theta)} \quad (14)$$

For the second factor in the right-hand-side (RHS) of (14), we can use a derivative formula given in [6]

$$\frac{dP_n^{|m|}(u)}{du} = -\frac{|m|u}{1-u^2} P_n^{|m|}(u) - \frac{P_n^{|m|+1}(u)}{(1-u^2)^{1/2}} \quad (15)$$

With that substitution, we obtain

$$\begin{aligned} \frac{dP_n^{|m|}(\cos \theta)}{d\theta} &= \frac{|m|u}{\sqrt{1-u^2}} P_n^{|m|}(u) + P_n^{|m|+1}(u) \\ &= \cos \theta \frac{|m| P_n^{|m|}(\cos \theta)}{\sin \theta} + P_n^{|m|+1}(\cos \theta) \end{aligned} \quad (16)$$

We again encounter  $P_n^{|m|}(\cos \theta)/\sin \theta$  factor in the RHS of (16) for which we can consult Table I for  $\theta \rightarrow 0, \pi$ . The only exception is for  $|m| = 1$  where the pre-multiplying factor is  $-|m| = -1$ .

The discussion above allows us to re-write (2), (3) as

$$e_{mn}^\theta = j^n \left[ \frac{P_n^{|m|}(\cos \theta)}{\sin \theta} (|m|Q_{2mn} \cos \theta - mQ_{1mn}) + Q_{2mn} P_n^{|m|+1}(\cos \theta) \right] \quad (17)$$

$$e_{mn}^\phi = j^{n+1} \left[ \frac{P_n^{|m|}(\cos \theta)}{\sin \theta} (mQ_{2mn} - |m|Q_{1mn} \cos \theta) - Q_{1mn} P_n^{|m|+1}(\cos \theta) \right] \quad (18)$$

### III. SIMPLE EXAMPLES

#### A. Single Hertzian dipole

1)  $+\hat{z}$ -directed Hertzian dipole with  $I\Delta l = 1$  Am at origin: This is a single  $\text{TM}_{m=0,n=1}$  mode. From FEKO,  $Q_{201} = -93.7 [\sqrt{W}]$ . We are left with

$$\vec{E}^{\text{ff}}(r, \theta, \phi) = \beta \sqrt{\frac{Z_0}{2\pi}} \frac{e^{-j\beta r}}{\beta r} \sqrt{\frac{3}{4}} e_{01}^\theta \hat{\theta} \quad (19)$$

where

$$\begin{aligned} e_{01}^\theta &= jQ_{201} P_1^1(\cos \theta) \\ &= jQ_{201} (-\sin \theta) \\ &= j93.7 \sin \theta [\sqrt{W}] \end{aligned} \quad (20)$$

The  $\sin \theta$  radiation pattern and  $\hat{\theta}$  only polarization are expected. Neglecting the  $e^{-j\beta r}/r$  factor (implicitly assumed henceforth) and using  $Z_0 = 367.73\Omega^1$ , we obtain  $\vec{E}^{\text{ff}}(\pi/2, 0) = j628.3 \hat{\theta}$  which is identical to  $j628.3$  given by FEKO.

2)  $+\hat{y}$ -directed Hertzian dipole with  $I\Delta l = 1$  Am at origin: From FEKO:  $Q_{2,-1,1} = Q_{211} = j66.25 [\sqrt{W}]$

$$\begin{aligned} \vec{E}^{\text{ff}}(r, \theta, \phi) &= \beta \sqrt{\frac{Z_0}{2\pi}} \frac{e^{-j\beta r}}{\beta r} \Sigma \\ \Sigma &= -e^{j\phi} \sqrt{\frac{3}{8}} (e_{11}^\theta \hat{\theta} + e_{11}^\phi \hat{\phi}) + e^{-j\phi} \sqrt{\frac{3}{8}} (e_{-11}^\theta \hat{\theta} + e_{-11}^\phi \hat{\phi}) \end{aligned} \quad (21)$$

where

$$\begin{aligned} e_{-11}^\theta &= -jQ_{2,-1,1} \cos \theta \\ e_{11}^\theta &= -jQ_{211} \cos \theta \\ e_{-11}^\phi &= -Q_{2,-1,1} \\ e_{11}^\phi &= Q_{211} \end{aligned} \quad (22)$$

substituting the values for  $Q_{2,-1,1}$  and  $Q_{211}$ , we obtain

$$\Sigma = -2j 66.25 \sqrt{\frac{3}{8}} (\cos \theta \sin \phi \hat{\theta} + \cos \phi \hat{\phi}) \quad (23)$$

Again,  $\vec{E}^{\text{ff}}(0, 0) = -j628.3 \hat{\phi}$  is identical to  $-j628.3$  given by FEKO.

3)  $+\hat{x}$ -directed Hertzian dipole with  $I\Delta l = 1$  Am at origin: From FEKO:  $Q_{2,-1,1} = -Q_{211} = 66.25 [\sqrt{W}]$ . Re-using (21) and (22), we obtain

$$\Sigma = -2j 66.25 \sqrt{\frac{3}{8}} (\cos \theta \cos \phi \hat{\theta} - \sin \phi \hat{\phi}) \quad (24)$$

Note that the patterns expressed in (23) and (24) are consistent with the Jones matrix of crossed  $\hat{x}$  and  $\hat{y}$  Hertzian dipoles [7].

<sup>1</sup>using  $\mu_0 = 4\pi 10^{-7}$  and  $\epsilon_0 = 8.854 10^{-12}$ . This more closely matches the value used in FEKO as opposed to  $377$  or  $120\pi \Omega$

### B. Array of Hertzian dipoles

Consider two Hertzian dipoles,  $+\hat{y}$ -directed at  $(0, 0, \lambda/20)$  and  $-\hat{y}$ -directed at  $(0, 0, -\lambda/20)$ , each with  $I\Delta l = 1$  Am. FEKO SWE coefficients for this problem are:  $-Q_{1,-1,1} = Q_{111} = 20.6$ ;  $Q_{2,-1,2} = Q_{212} = j15.9$ ;  $-Q_{1,-1,3} = Q_{113} = 0.089$ . We neglect  $-Q_{1,-1,3}, Q_{113}$  (very small) values for simplicity.

It can be shown that

$$\begin{aligned} \Sigma &\approx \frac{C_{11}}{\sqrt{2}} \left( [e_{-11}^\theta e^{-j\phi} - e_{11}^\theta e^{j\phi}] \hat{\theta} + [e_{-11}^\phi e^{-j\phi} - e_{11}^\phi e^{j\phi}] \hat{\phi} \right) + \\ &+ \frac{C_{12}}{\sqrt{6}} \left( [e_{-12}^\theta e^{-j\phi} - e_{12}^\theta e^{j\phi}] \hat{\theta} + [e_{-12}^\phi e^{-j\phi} - e_{12}^\phi e^{j\phi}] \hat{\phi} \right) \end{aligned} \quad (25)$$

Substituting the coefficients, we obtain

$$\Sigma \approx 50.4 \cos \theta \left( \cos \theta \sin \phi \hat{\theta} + \cos \phi \hat{\phi} \right) \quad (26)$$

This radiation pattern is proportional to  $\cos \theta$  times (23). The  $\cos \theta$  factor can be seen as the array factor of two closely spaced and oppositely signed point sources:  $\sin([\beta\lambda/20] \cos \theta) \approx [\beta\lambda/20] \cos \theta$ . Here,  $\vec{E}^{\text{ff}}(0, 0) = 390 \hat{\phi}$  which is similar to 388.3 given by FEKO. This small difference seems to be due to the neglected  $Q_{1,-1,3}, Q_{113}$  factors.

## IV. NUMERICAL IMPLEMENTATION AND EXAMPLES

### A. Implementation

We find equations (17) and (18) in conjunction with (1) to be very convenient for numerical implementation. Two aspects are worth mentioning:

- 1) FEKO \*.out file prints (“FAR FIELD MODAL COEFFICIENTS”)  $Q_{1mn}$  and  $Q_{2mn}$  alternately (as a column vector) with increasing order  $m = -n$  to  $n$  for every degree  $n$ . Once the  $Q_{1mn}$  and  $Q_{2mn}$  are separated into two column vectors, the FEKO  $(m, n)$  format is convenient as it is compatible with **legendre(n,u)** function found in MATLAB.
- 2)  $P_n^{|m|}(\cos \theta)/\sin \theta$  and  $P_n^{|m|+1}(\cos \theta)$  are easily implemented using **legendre(n,u)**. We deal with apparent singularities in the former as per Tab. I.
- 3) Numerical calculation of the factorials in (11) appears to be unstable for  $N \sim > 45$ . Consequently, we employ forward and backward differencing to approximate (8) numerically.

### B. Example: closely spaced $\pm\hat{y}$ Hertzian dipoles

We return to the example in Sec. III-B, this time testing our numerical implementation. All FEKO SWE coefficients including  $Q_{1,-1,3} = Q_{113}$  are used. The analytical expression for this problem is:

$$\vec{E}^{\text{ff}}(\theta, \phi) = 2 \frac{I\Delta l}{4\pi} Z_0 \beta \sin(2\pi \frac{z}{\lambda} \cos \theta) \left( \cos \theta \sin \phi \hat{\theta} + \cos \phi \hat{\phi} \right) \quad (27)$$

where  $I\Delta l = 1$  Am and  $z/\lambda = 1/20$ .

Fig. 1 reports comparison between analytical expression and numerical calculation based on spherical harmonics for the  $(\theta, \phi)$  trajectory indicated. This trajectory is representative of of a celestial source, Hydra, as seen from the Murchison Radio-astronomy Observatory (MRO) in Western Australia. The difference between the two curves of less than 0.25% is very small.

### C. Example: Antenna Array on Soil

The next example is a pseudo random array of 16 dual-polarized log-periodic antennas (referred to as AAVS0.5) on MRO soil [8], [9]. Fig. 2 depicts the simulation setup in FEKO. The array is pointed to Azimuth/Elevation of 0/75 degrees. Fig. 3 reports antenna gains at the nominal pointing direction taken from FEKO far-field data and computed via spherical harmonics over frequency. The two results are in excellent agreement with no more than  $\sim 0.5\%$  difference.

## V. CONCLUSION

Spherical harmonics expansion is a convenient method for calculating continuous far-field radiation. This is especially useful in radio astronomy where celestial sources follow trajectories that continuously vary in  $\theta, \phi$  in the spherical coordinate system. We discussed an implementation based on FEKO generated spherical modal coefficients and found very good agreement with far-field values calculated by FEKO and analytical expression.

## ACKNOWLEDGMENT

The author thanks D. Ung, T. Colegate, and S. Padhi for setting up FEKO simulations for AAVS0.5.

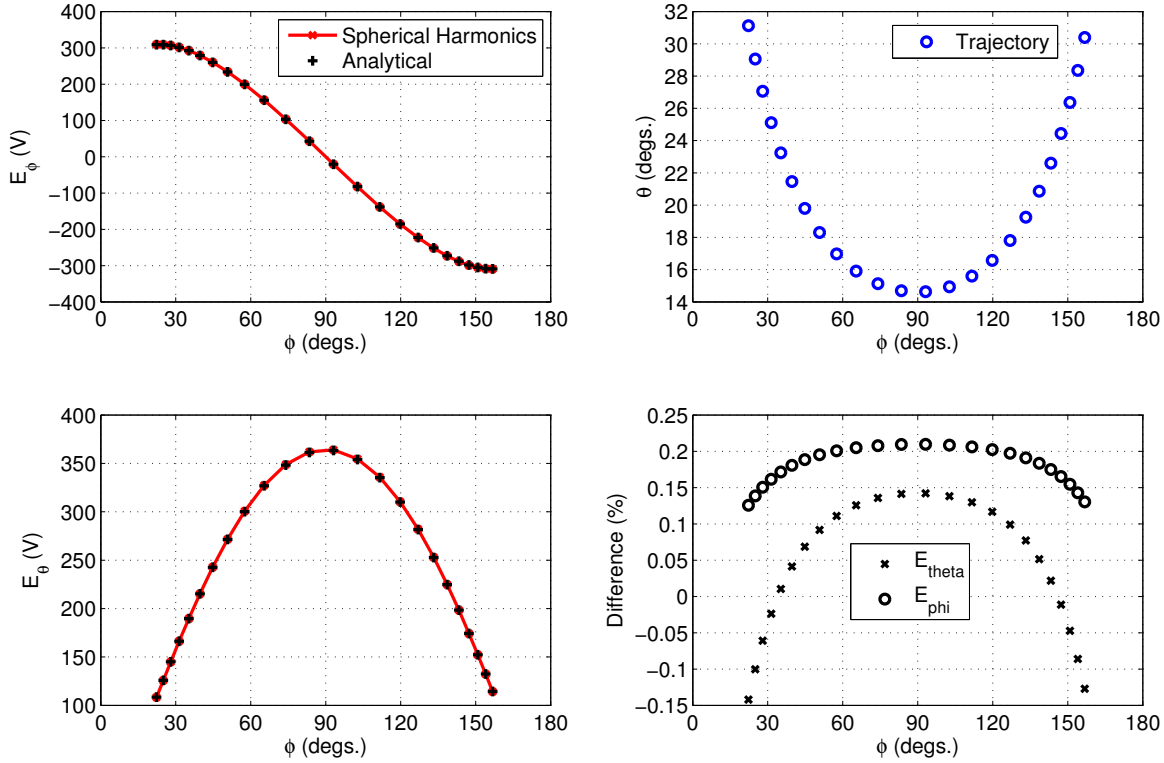


Figure 1. Comparison between numerically calculated far-field based on spherical harmonics and analytical expression. The difference is less than 0.25%.

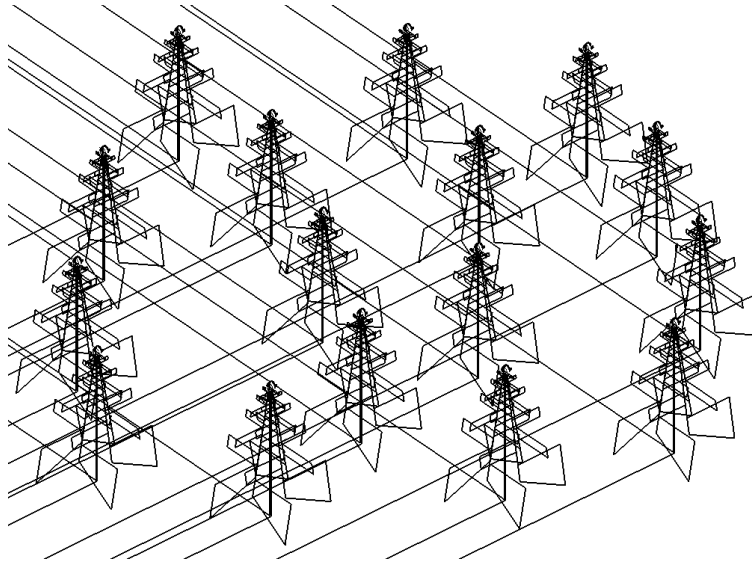


Figure 2. FEKO simulation of a pseudo random array of 16 dual-polarized log-periodic antennas distributed in an 8 m diameter circle.

## REFERENCES

- [1] FEKO, *14.20 AS Card*, user manual.
- [2] Y. Chen and T. Simpson, "Radiation pattern analysis of arbitrary wire antennas using spherical mode expansions with vector coefficients," *Antennas and Propagation, IEEE Transactions on*, vol. 39, no. 12, pp. 1716–1721, Dec 1991.
- [3] P. Koivisto, "Reduction of errors in antenna radiation patterns using optimally truncated spherical wave expansion," *Progress In Electromagnetics Research*, vol. 47, pp. 313–333, 2004.
- [4] J. Rahola, F. Belloni, and A. Richter, "Modelling of radiation patterns using scalar spherical harmonics with vector coefficients," in *Antennas and Propagation, 2009. EuCAP 2009. 3rd European Conference on*, March 2009, pp. 3361–3365.

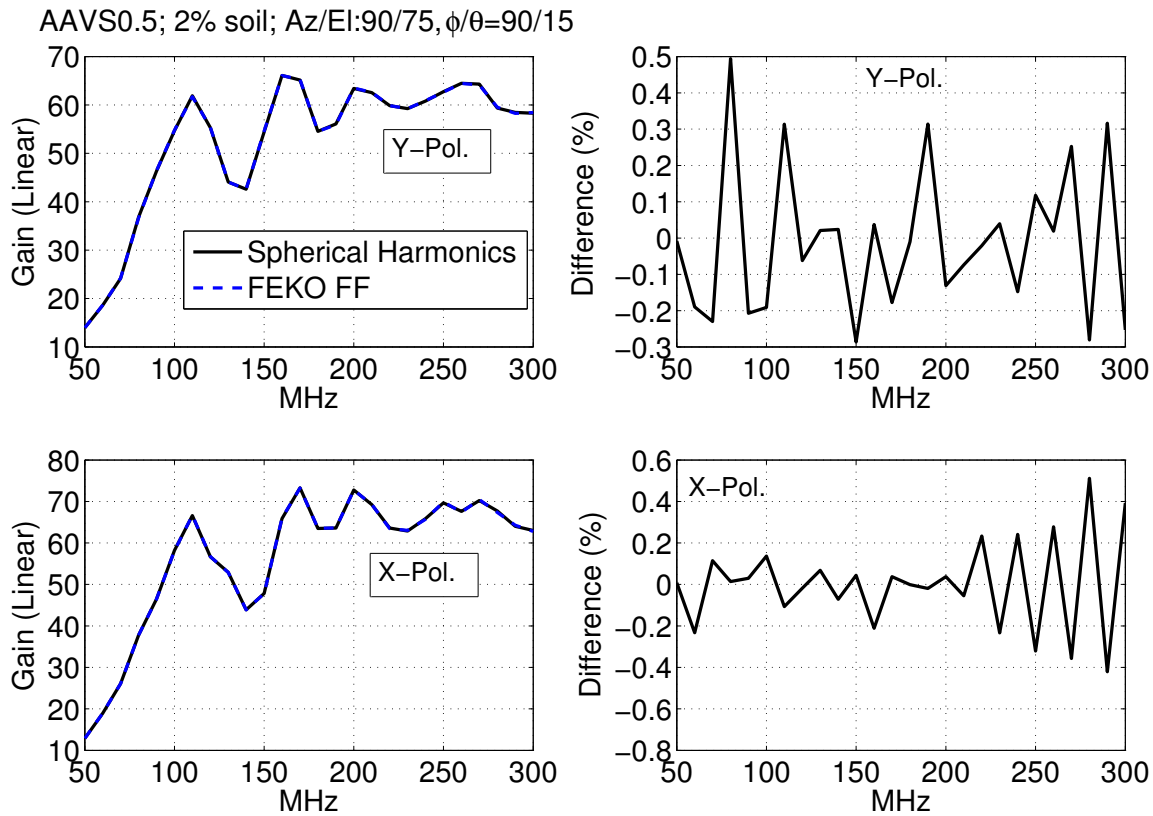


Figure 3. Antenna gains for Y (N-S) and X (E-W) polarization taken from FEKO far-field data and calculated from spherical wave expansion.

- [5] R. F. Harrington, *Time-Harmonic Electromagnetic Fields*. Wiley-Interscience, 2001, ch. 6.
- [6] —, *Time-Harmonic Electromagnetic Fields*. Wiley-Interscience, 2001, appendix E.
- [7] A. Sutinjo, J. O’Sullivan, E. Lenc, R. B. Wayth, S. Padhi, P. Hall, and S. J. Tingay, “Understanding instrumental Stokes leakage in Murchison Widefield Array polarimetry,” *Radio Science*, vol. 50, no. 1, pp. 52–65, 2015, 2014RS005517. [Online]. Available: <http://dx.doi.org/10.1002/2014RS005517>
- [8] P. Hall, A. Sutinjo, E. de Lera Acedo, R. Wayth, N. Razavi-Ghods, T. Colegate, A. Faulkner, B. Juswardy, B. Fiorelli, T. Booler, J. de Vaate, M. Waterson, and S. Tingay, “First results from AAVS 0.5: A prototype array for next-generation radio astronomy,” in *Electromagnetics in Advanced Applications (ICEAA), 2013 International Conference on*, 2013, pp. 340–343.
- [9] T. Colegate, A. Sutinjo, P. Hall, S. Padhi, R. Wayth, J. bij de Vaate, B. Crosse, D. Emrich, A. Faulkner, N. Hurley-Walker, E. de Lera Acedo, B. Juswardy, N. Razavi-Ghods, S. Tingay, and A. Williams, “Antenna array characterization via radio interferometry observation of astronomical sources,” in *Antenna Measurements Applications (CAMA), 2014 IEEE Conference on*, Nov 2014, pp. 1–4.